Submitted to Gmelin Institute, ~~July~~ Sept. 1963

A-66a(BC63)

NOV 18 1963

BNL 7375

Automatic Bubble Density Measurement with the Hough-Powell System*

R.C. Strand, A.M. Thorndike, and N.W. Webre

MASTER

April 25, 1963

The Brookhaven Bubble Chamber Group is developing a Hough-Powell fast analysis system (HPD)[1] for bubble chamber photographs. High precision measurements are made with a computer controlled flying spot digitizer. We are currently testing the track selection programs for the system. We have just completed a study of a method for automatic bubble density measurements.

Bubble density measurements are useful to identify particles and thereby reduce the number of ambiguous kinematic fits for a bubble chamber event. An accurate determination of bubble density is tedious and time consuming by the individual gap length method. The HPD bubble density measurements are obtained along with the geometry points at a rate of about six seconds per twenty-inch chamber photograph.

We will describe the HPD and its bubble density measurement process before we present the results of our recent tests.

The HPD employs a mechanical flying spot with associated optical and electronic elements that are capable of reducing the information content of a bubble chamber photograph to precise digital form. The first two figures will show how this is done. Figure 1, a view of the 20-inch

---

*Work performed under the auspices of the United States Atomic Energy Commission.

LEGAL NOTICE

This report was prepared as an account of Government sponsored work. Neither the United States, nor the Commission, nor any person acting on behalf of the Commission:

A. Makes any warranty or representation, expressed or implied, with respect to the accuracy, completeness, or usefulness of the information contained in this report, or that the use of any information, apparatus, method, or process disclosed in this report may not infringe privately owned rights; or

B. Assumes any liabilities with respect to the use of, or for damages resulting from the use of any information, apparatus, method, or process disclosed in this report.

As used in the above, "person acting on behalf of the Commission" includes any employee or contractor of the Commission, or employee of such contractor, to the extent that such employee or contractor of the Commission, or employee of such contractor prepares, disseminates, or provides access to, any information pursuant to his employment or contract with the Commission, or his employment with such contractor.

Facsimile Price $ 1.60

Microfilm Price $ .80

Available from the
Office of Technical Services
Department of Commerce
Washington 25, D. C.

DISCLAIMER

This report was prepared as an account of work sponsored by an agency of the United States Government. Neither the United States Government nor any agency Thereof, nor any of their employees, makes any warranty, express or implied, or assumes any legal liability or responsibility for the accuracy, completeness, or usefulness of any information, apparatus, product, or process disclosed, or represents that its use would not infringe privately owned rights. Reference herein to any specific commercial product, process, or service by trade name, trademark, manufacturer, or otherwise does not necessarily constitute or imply its endorsement, recommendation, or favoring by the United States Government or any agency thereof. The views and opinions of authors expressed herein do not necessarily state or reflect those of the United States Government or any agency thereof.

DISCLAIMER

Portions of this document may be illegible in electronic image products. Images are produced from the best available original document.

hydrogen chamber, exposed to 900 Mev positive pions at the AGS, shows the external fiducials used for rough digitizing at the bottom and the binary data box at the left. The smaller X's in the picture are fiducials for the geometry program. This photograph was read by the HPD which transmitted the coordinates of all hits on bubble images into an IBM 7090 computer. The 7090 CRT display of this data appears in Figure 2. The horizontal scale is stretched by a factor of four-thirds for plotting convenience. We see that the picture is honestly reproduced and that variations in bubble density are reproduced.

For the present, event pattern recognition is provided by humans. In Figure 3 we see a scanner making road measurements of an event of interest. All information which lies outside of the roads determined by the rough measurements is discarded by the computer. The centrally located two-prong event in Figure 1 was processed. Some of the hits in the beam track road are shown in Figure 4.

The dots are the road points selected for the track by the FILTER subroutine. The solid squares are background points and the solid triangles are averaged points. Figure 5 shows two tracks in the road and a crossing track.

Returning to bubble density, we expect that the lengths of gaps in a track form a Poisson distribution. Adjacent bubbles frequently coalesce into continuous elements or blobs. If we consider a bubble to be the smallest possible blob, then a track consists of many blobs separated by an equal number of gaps. We combine the flying spot size and the bubble image size into an equivalent HPD scan width, a, for which bubbles can be treated as points. For a track of mean bubble density, k, per micron on the film

$$e^{-ka}$$

is the probability that a miss will occur on a single sweep across the track.

We assume that neither energy loss nor dip angle cause any change in the bubble density over the segment under consideration. We assume that there are no background bubbles near the track. In practice this means that we must turn off the bubble density measurement whenever the track is obscured.

A maximum likelihood estimate of the mean bubble spacing, λ, is given by equation (1)

$$\lambda = s/\ln\left(\frac{M}{M-C}\right) \qquad (1)$$

where s is the scan line separation

M is the total number of Misses

C is the total number of gaps.[2]

In this case there is the additional requirement that

$$a/2 < s < a$$

so that at most one bubble could be digitized only twice. This condition is compatible with the requirements of measurement speed and the FILTER subroutine.

To test the HPD bubble density measurement, we plotted all of the road points for the beam track of the two-prong event in Figure 1. By eye, we selected the hits which were associated with the track and we determined whether a hit or miss occurred on each scan of the track. We plotted the hit-miss structure of the track as shown in Figure 6. For this track we found 68 data cells and 244 misses. The scan line separation was 28 microns and from equation (1) the inverse bubble density, λ , was found to be 86 ± 11 microns. The error is purely statistical. The same track was measured on one of the bubble chamber group's measuring projectors by

our conventional gap measurement method. This yielded

$\lambda_{\parallel} = 83 \pm 8$ microns

Again, the error is statistical.

Recently Neil Webre included automatic bubble density measurement in the FILTER subroutine. Some of the 900 Mev π^+ events were processed. Due to FILTER difficulties it was necessary to follow the computation in detail. We present results for 9 selected tracks that were FILTERed properly. These tracks were also measured on the measuring projector for comparison. The data appears in Table I. The first three tracks in Table I are minimum beam tracks. The remaining tracks cover the range to about five times minimum. Agreement with the results from the measuring projector is poor for the dense tracks. This is thought to be due to our computing the number of misses from the difference between the total number of scans and the total number of hits. We will change this computation to a direct tally of the number of misses. This will greatly reduce the measurement error for dense tracks.

We conclude from measuring the same track repeatedly, that the reproducibility of HPD bubble density measurement is currently of the same order of magnitude as the statistical error. This is mostly caused by the ± 5% regulation of the speed of the moving stage. We expect to reduce this to ± 2%.

Figures 7, 8, and 9 are bubble chamber photographs of some of the tracks that were measured. The HPD mean bubble formation lengths for these tracks are indicated on the figures.

As a result of these tests, we feel that high quality bubble density measurements will be provided by the HPD system.

References

1. Paul V.C. Hough. A Method for Faster Analysis of Bubble Chamber Photographs. Proceedings of an International Conference on Instrumentation for High Energy Physics (University of California at Berkeley, 1961), p. 242

2. R.C. Strand. Bubble Density Measurement with the Hough-Powell Digitizer. BNL Bubble Chamber Report C-34, January 1963.

TABLE I

MEAN GAP DATA

Meas. Proj.	HPD
50 ± 5 μ	48 ± 6
59 ± 5	59 ± 9
50 ± 4	67 ± 8
10 ± 2	26 ± 4
20 ± 2	23 ± 3
28 ± 2	27 ± 3
50 ± 3	49 ± 4
41 ± 3	39 ± 3
21 ± 3	24 ± 3

Figure Captions

Fig. 1. A BNL 20 inch hydrogen chamber photograph. The chamber was exposed to 900 Mev positive pions which enter the chamber at the bottom of the page. The centrally located two-prong event was found to be an elastic collision.

Fig. 2.. The HPD digital reproduction of a BNL 20 inch hydrogen chamber photograph. This is a photograph of the CRT plot of the HPD digital measurement of the picture in Fig. 1. The horizontal scale has been stretched by a factor of four-thirds for plotting convenience.

Fig. 3. A rough digitizing scanner for making HPD "roads". Fiducials and three points on each track are digitized. The HPD control program uses these measurements to exclude the unwanted portions of the picture.

Fig. 4. HPD FILTERed tracks. One track, designated by the dots, lies in the road. Background hits are shown by squares. Two groups of twenty hits each are shown. The last hit in each group is indicated by an open figure. The average dot for each group is shown as a solid triangle.

Fig. 5. HPD FILTERed tracks. The first group of twenty hits shows two roughly parallel tracks in the road. The second group shows a crossing track.

Fig. 6. Bubble density representation of a track.

Fig. 7. Automatic HPD bubble density measurement of track number one.

Fig. 8. Automatic HPD bubble density measurement of track number one.

Fig. 9. Automatic HPD bubble density measurement of tracks number zero and number one.

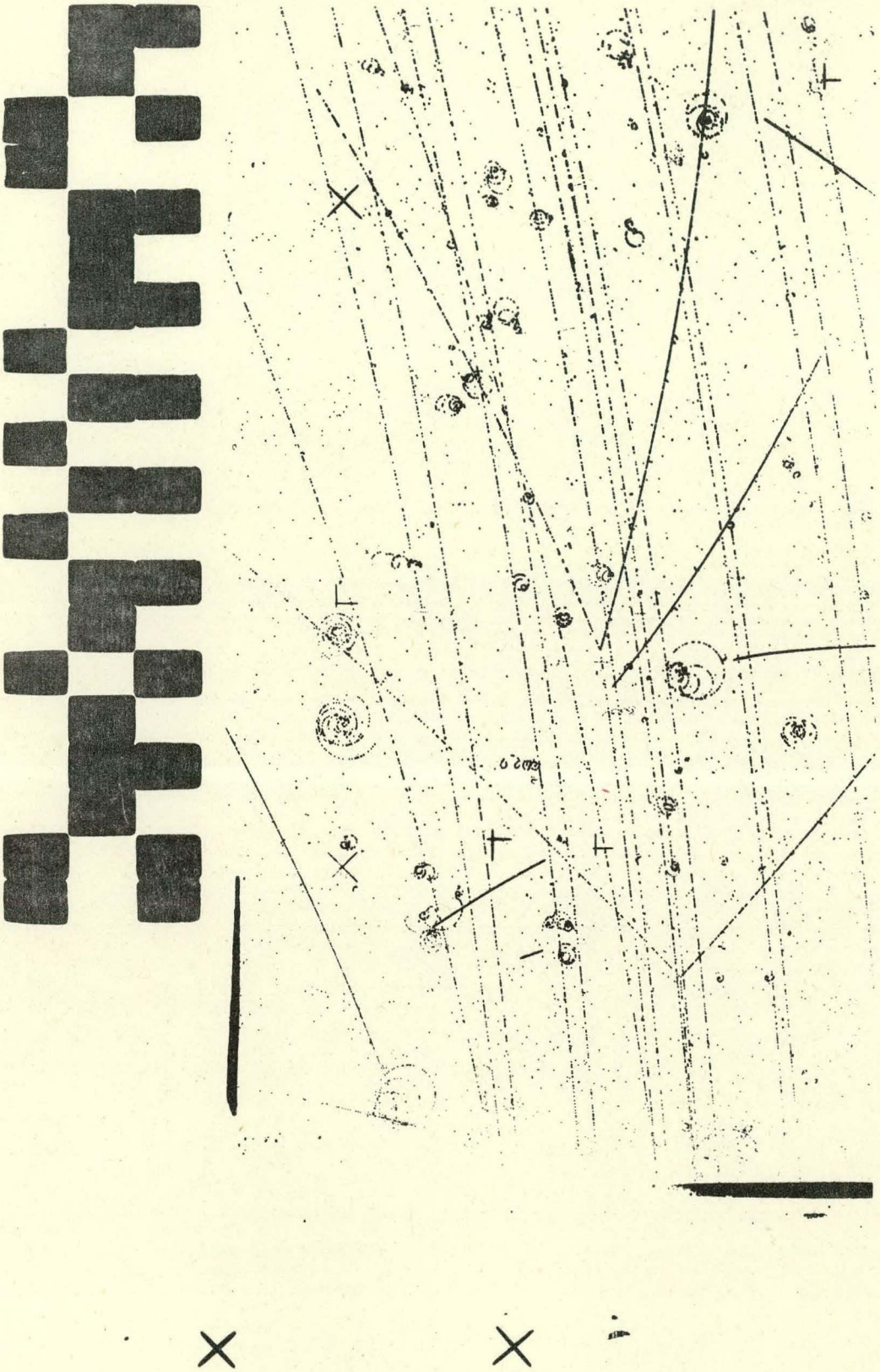

FIGURE 1

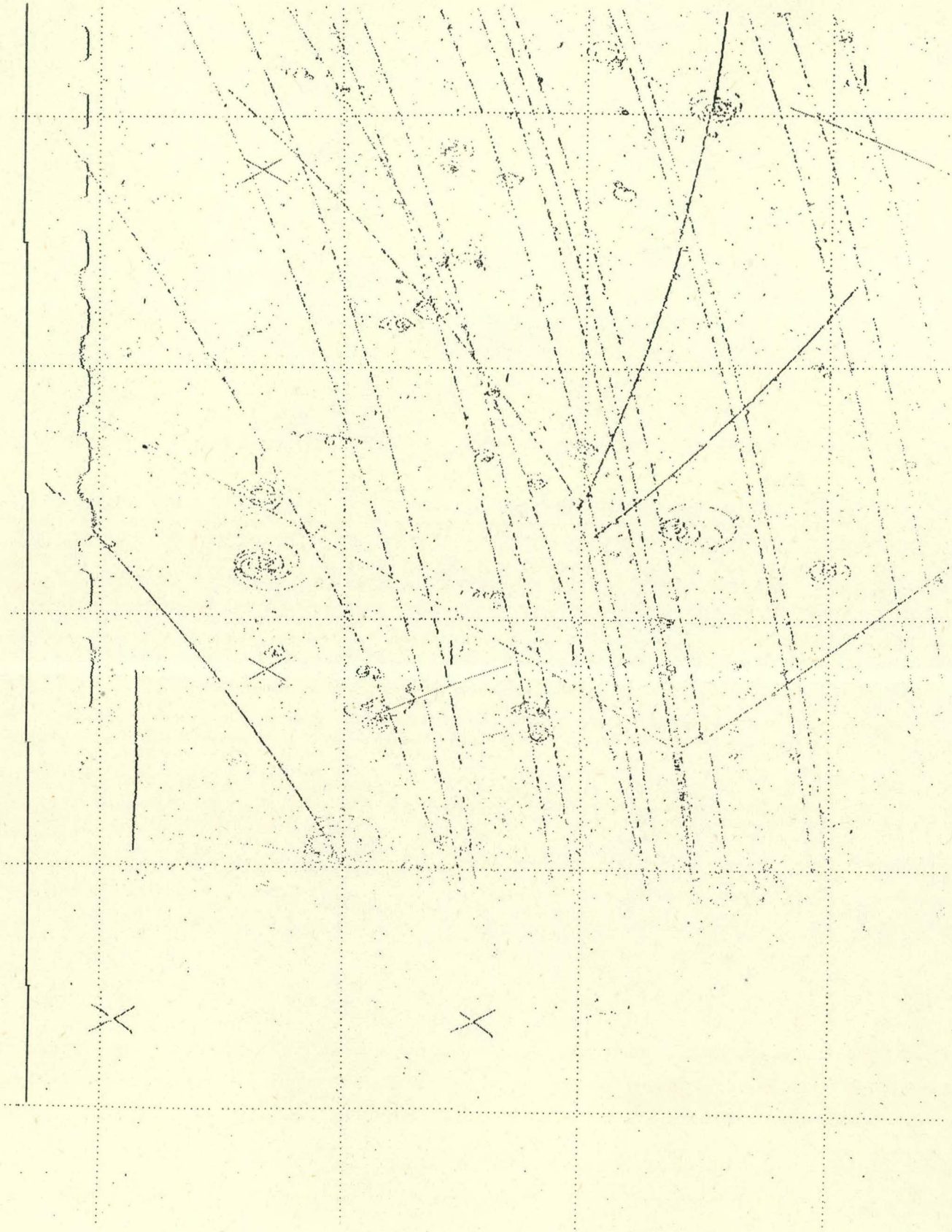

FIGURE 2

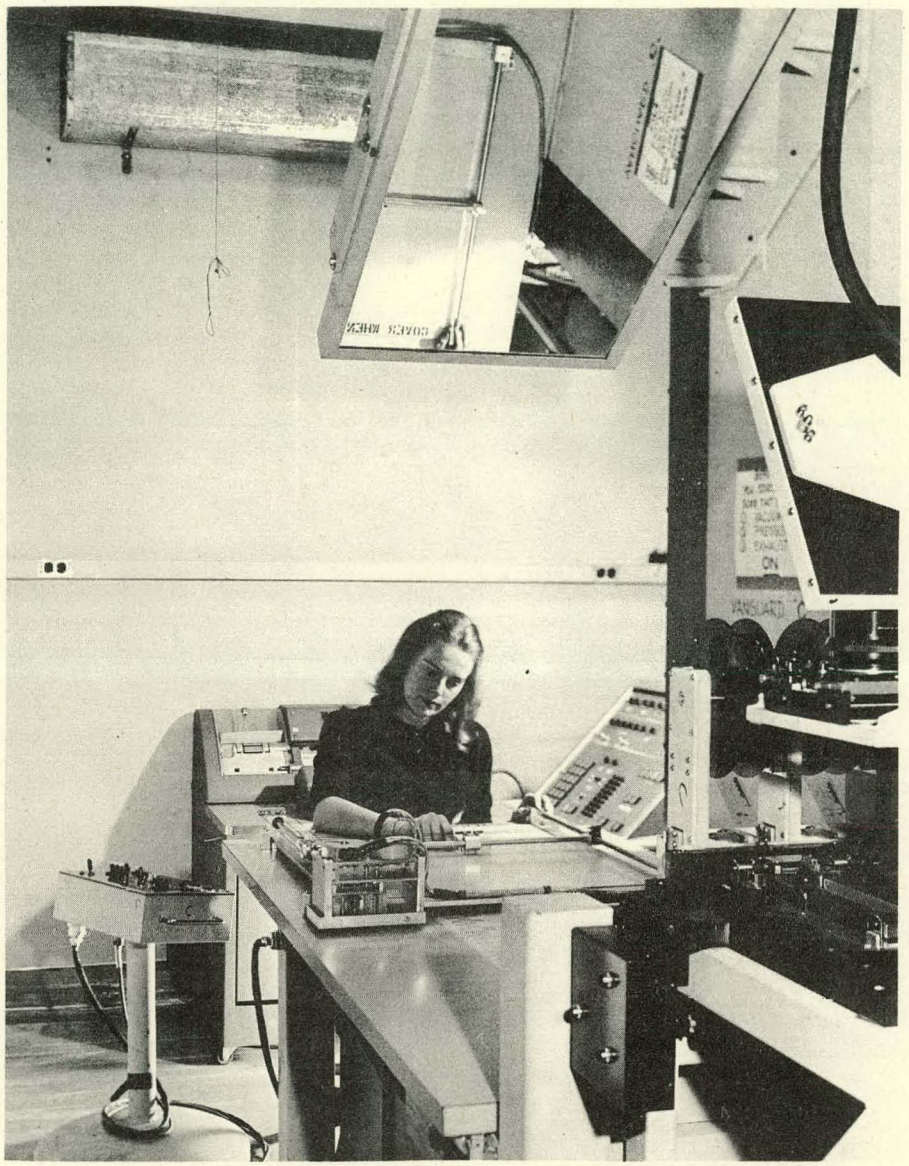

FIGURE 3

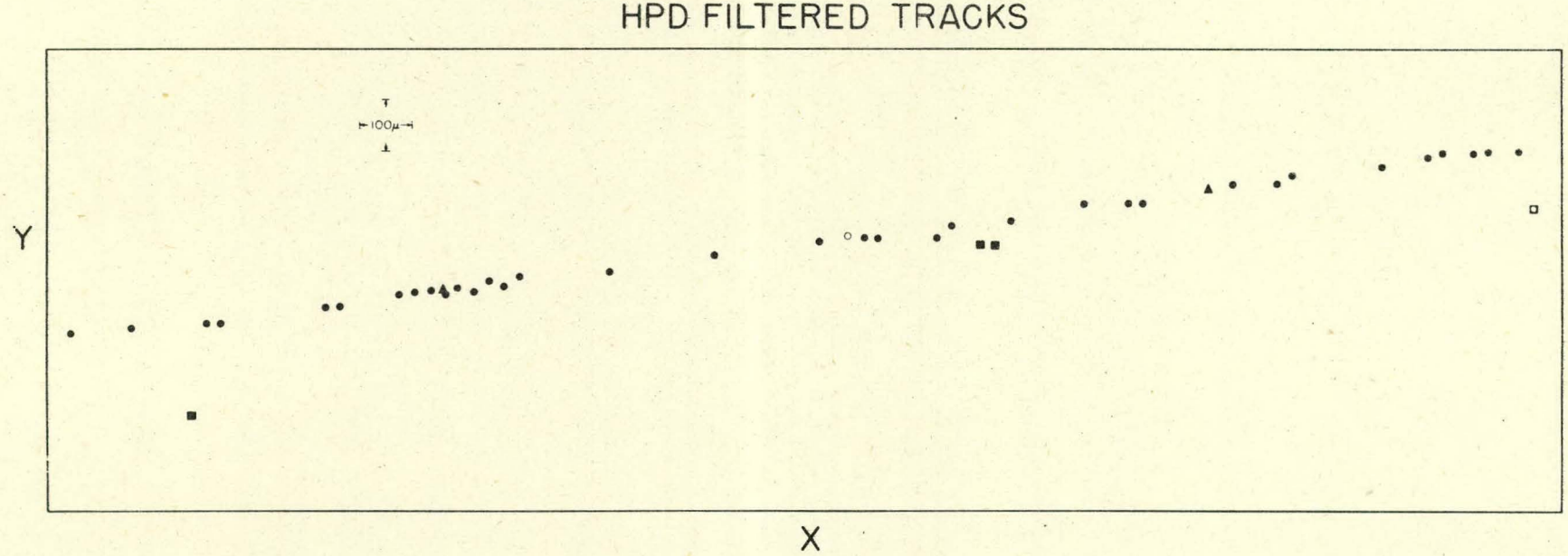

FIGURE 4

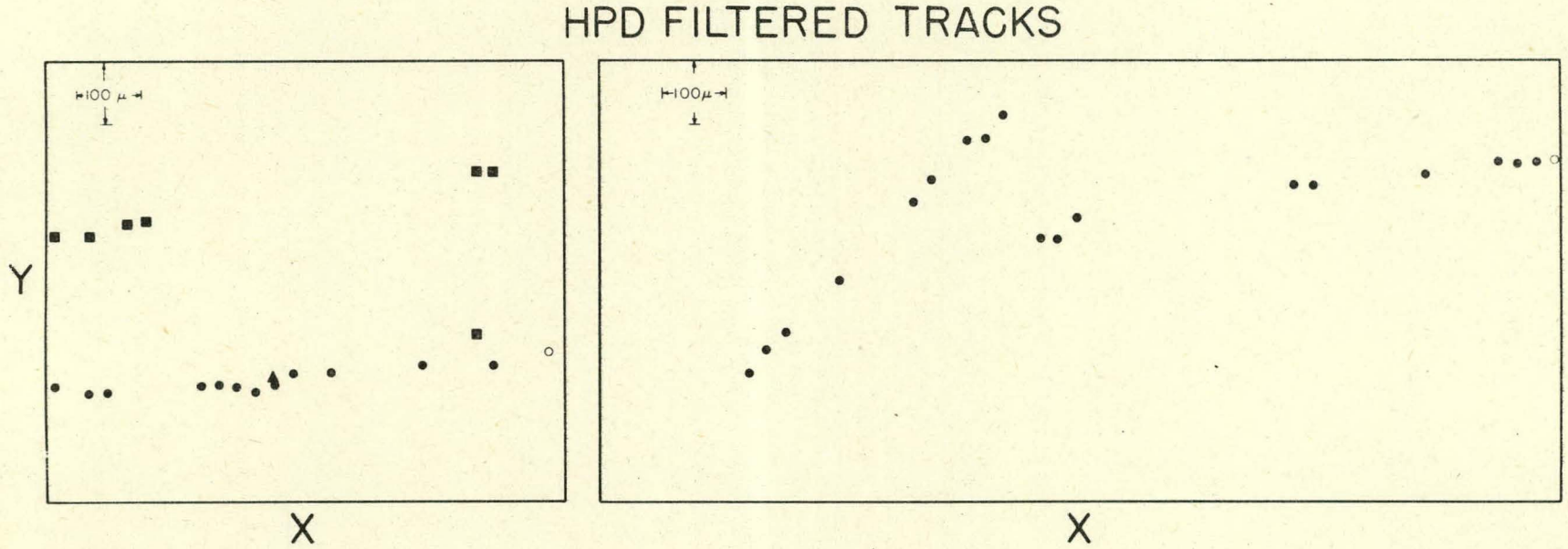

FIGURE 5

BUBBLE DENSITY REPRESENTATION OF A TRACK

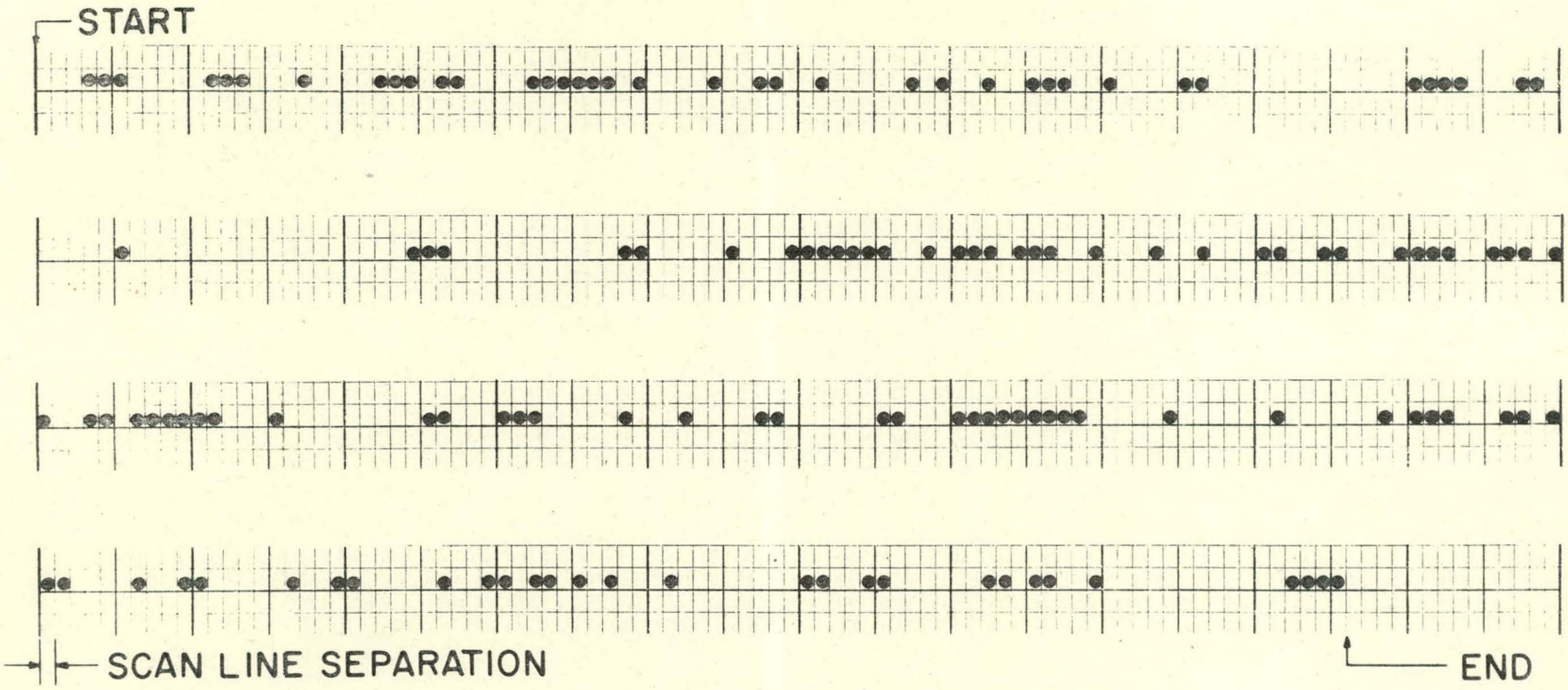

FIGURE 6

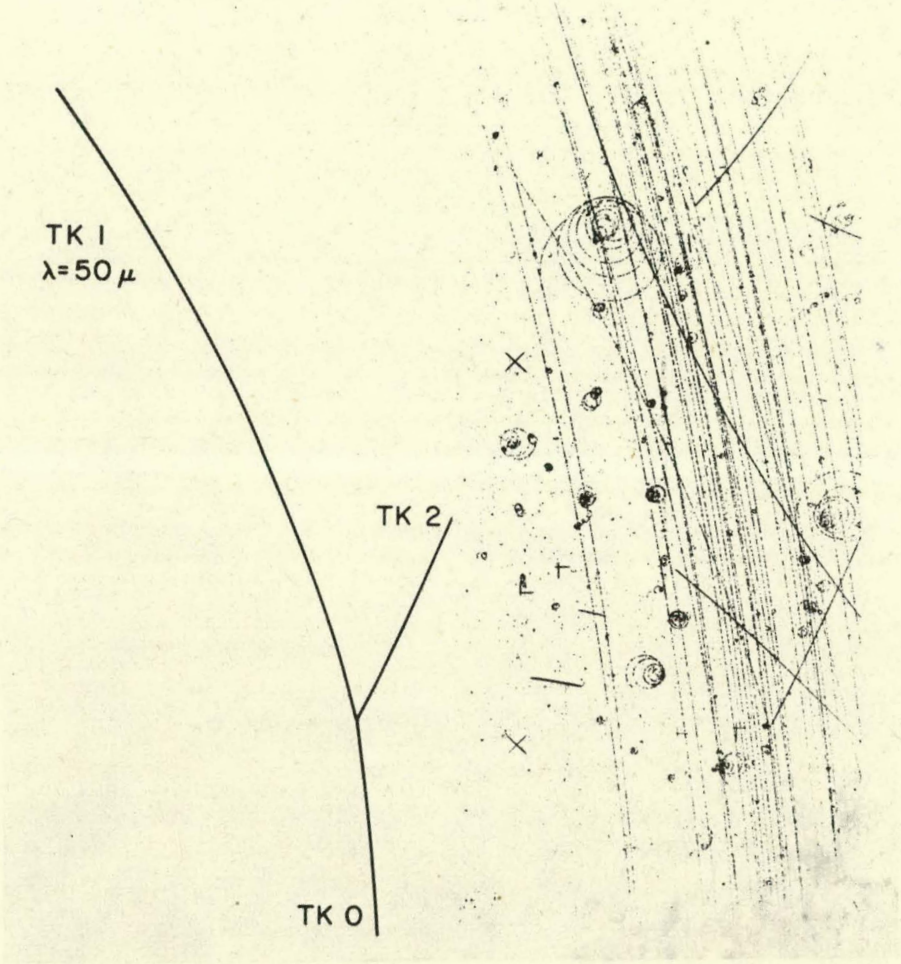

FIGURE 7

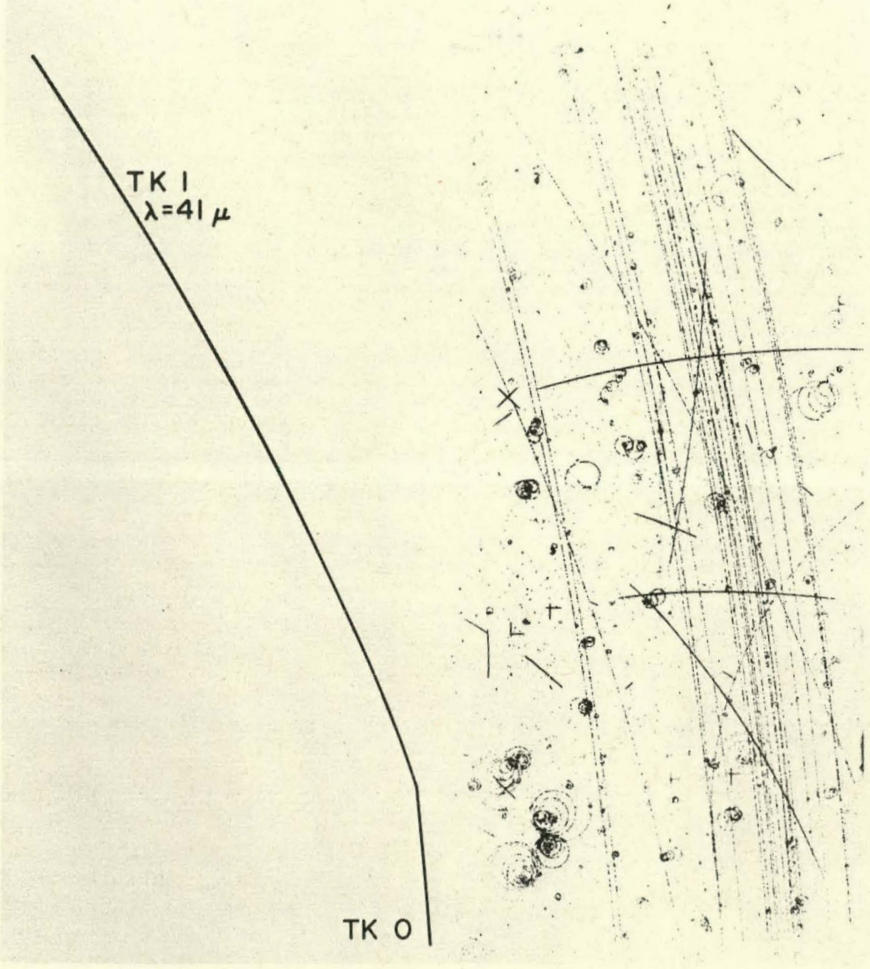

FIGURE 8

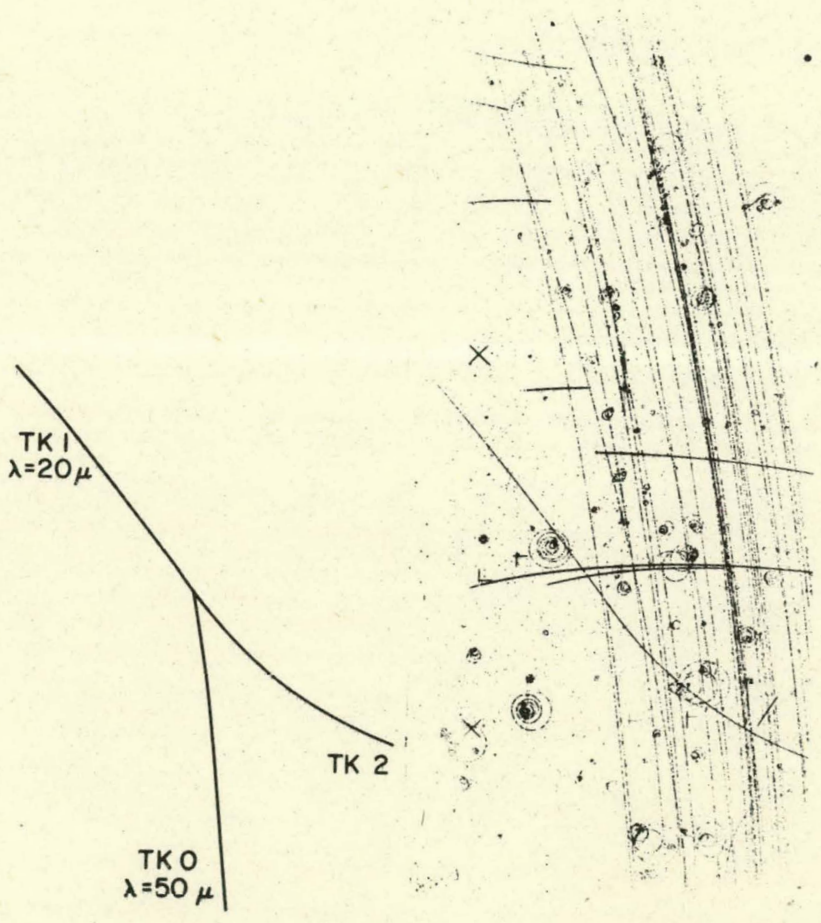

FIGURE 9